

Numerical Simulation of Aerospike Nozzle Inviscid Isentropic Flowfield

K. M. Khan¹, S. Khushnood²

¹Department of Mechanical Engineering, University of Engineering and Technology, Taxila, Pakistan

²Department of Mechanical Engineering, University of Engineering and Technology, Taxila, Pakistan
kmkhan89@yahoo.com

Abstract: The flowfield established on the axisymmetric aerospike/plug nozzle in quiescent air is explored numerically. Nozzle profiles have been constructed using the canonical FORTRAN programs. Inviscid flow analysis has been performed using FLUENT package to qualify the plug nozzle flowfield. Study and investigation of the following configurations have been performed. Internal-external expansion full-length contoured case. External-expansion contoured full-length and truncated cases. Internal-external expansion conical full-length and truncated cases. Theory and simulation results show agreement in some cases. There are disagreements that require further investigations.

[K. M. Khan, S. Khushnood. **Numerical Simulation of Aerospike Nozzle Inviscid Isentropic Flowfield**, *Life Sci J* 2013;10(3):1340-1349] (ISSN: 1097-8135). <http://www.lifesciencesite.com>. 201

Keywords: Flowfield, Plug, Nozzle, Numerical, Inviscid, FLUENT

1. Introduction

Currently, rocket engines use the traditional convergent-divergent nozzle invented by Carl Patrick Gustaf de Laval in 1882. A convergent-divergent nozzle expands its exhaust optimally only to the ambient pressure for which it is designed. This is called point design [1] i.e., it overexpands if the ambient pressure is more than the design pressure and it underexpands if the ambient pressure is less than the design pressure [2, 3]. For given chamber pressure and temperature, and a particular gas or gamma, the nozzle has to change area ratio continuously to operate optimally in an environment with ambient pressure that changes from maximum at sea level to near vacuum in space [4, 5]. Large area-ratio bell nozzles operating at sea-level produce exhaust accompanied by flow separation resulting in performance losses, and nozzle structural failure due to dynamic loads [6]. A convergent-divergent nozzle engine is joined to the launcher by a thrust frame [7] which adds to dry mass. Steering is provided through gimbaling [8] which increases engine complexity and weight. There is a nozzle engine — the aerospike nozzle — that achieves better performance overall [9, 10, 11, 12] by adjusting almost optimally the “effective area ratio” to the change in altitude. This is called altitude adaptation/compensation [13]. The altitude compensation capability makes such nozzles more efficient than conventional nozzles over a wide range of ambient pressure variation [13, 14]. The name aerospike or plug for this type of nozzle is interchangeable [15]. The aerospike nozzle integrates nicely with the launcher aft body [16] both to reduce drag and to impart smooth thrust. It controls pitch,

yaw and roll only by switching the thrusters on and off [17]. The altitude compensating feature also allows the use of a simple, low-risk, gas generator cycle in aerospike engine. Instead of recirculation and burning the turbine exhaust, as in the Space Shuttle Main Engine (SSME), or dumping the exhaust over-board, as in most other bell-nozzle engines, the aerospike nozzle engine can be designed to channel the turbine exhaust to exit at the truncated base as base-bleed [18] and contribute to thrust. The nozzle interior accommodates much of the gas generator cycle hardware within it [19] and the whole nozzle system, as one piece, occupies the launcher base to reduce drag [20]. Failure of a few thrusters does not jeopardize the whole mission [21]. Aerospike nozzles can be circular or linear depending on the ramp shape. The original design was a circular or annular aerospike, which featured a plug-like ramp. The linear-type aerospike is a two-dimensional version of the annular type. The linear version has a “V” shape forming an edge at the thin end whereas the thick end accommodates the thrusters. Instead of expanding combustion gases internally along solid walls, the aerospike nozzle expands the gases externally either along an annular or a linear spike. Modern aerospike nozzle engine design is a mating of the conventional bell nozzle for much of the design expansion while the basic aerospike ramp serving to complement the expansion process. The aerospike engine is fully reusable and as part of a Single-Stage-To-Orbit (SSTO) design offers mechanical simplicity due to “single stage” [11]. The full-length aerospike is truncated to reduce weight and length without compromising much on thrust as the cut-away portion

is taken up by the aerodynamic spike. The linear aerospike nozzle is ideally suited for the lifting-body SSTO RLV (reusable launch vehicle). Research on rocket engines known to possess altitude adaptation/compensation features began in late 50's [22, 23] in an effort to cut mission costs and to improve the payload capability. NASA joined such efforts in the 60's to ascertain if the concept was practicable for the proposed Space Shuttle scheduled to be launched in early 80's. The truncated aerospike/plug nozzle was considered and tested for possible use on the Saturn-V and then later for the Space Shuttle Main Engines (SSME). Conventional bell-type nozzle was finally chosen because the technology was well-established [24]. Work on aerospike/plug nozzles significantly reduced in the early 1970s [14]. Complex geometry, flow physics [25] and materials of the time, not up to it, hindered plug nozzle use in rockets. Recent revival in aerospike/plug nozzle research came in 1990s when Lockheed Martin won the NASA contract for developing the SSTO technology demonstrator, X-33. NASA experimental demonstrator program, X-33, was cancelled [26] in 2001 as although the innovative aerospike engine cleared its test with performance reported as "textbook", the hydrogen fuel tank failed. Much of the SSTO promise for providing economically feasible alternative to conventional launchers hinged on lightweight launcher components. Fuel tank failure, in fact, drew the rug out from under the whole concept of SSTO. At California State University Long Beach (CSULB), a group of students and the faculty with the help of Garvey Spacecraft Corporation have done extensive research on liquid-propelled, clustered aerospike engines [27].

The plug nozzle concept is sensitive to any contour deviation from the ideal one, resulting in performance losses [15, 26]. Initial investigations of plug nozzle started with finding the nozzle contour that produced the best possible thrust. Theory provides ideal solution with the assumptions that the flow is inviscid and isentropic, i.e., it is perfect taken together from both fluid mechanics and thermodynamics points of view. Following this approach, the most simple plug nozzle contour is determined by the Prandtl-Meyer (P-M) flow expansion theory. Early FORTRAN programs to analyze flowfield of aerospike nozzle are now in public domain [28, 29]. The programs have been re-written to run on the Lahey/Fujitsu FORTRAN 95 language system integrated with MS Visual Studio IDE (Integrated Development Environment). An axisymmetric plug profile is either contoured or conical. In the present paper, the conical profile has been constructed by

joining with a straight line the end points of the curve for the contoured profile. Both cases have been simulated using FLUENT to establish the extent to which CFD follows the P-M theory.

2. Theoretical Background and Methodology

The Navier-Stokes equations (NSEs) were formulated in the early 1800's independently by M. Navier in France and G. G. Stokes in England. The equation set represents a system of unsteady, nonlinear, coupled, partial differential equations that relate pressure, temperature, density and velocity of a fluid in space and time. The Euler equations can be obtained by dropping the viscous terms in the NSEs. No analytical solution of either the Euler equation set or the NSEs [30] is available at present. Powerful computers are used to solve the approximations to the equation set by using discretization techniques like finite difference, finite volume, finite element and spectral methods. Many NSEs solvers are in existence like NPARC, PAB, WIND and FLUENT. FLUENT solves the Navier-Stokes equations by finite volume method. It employs control-volume technique by dividing the domain into discrete volumes (three-dimensional case), called cells, forming the computational grid. Integration of the NSEs on each cell center gives a set of nonlinear coupled algebraic equations for the flow variables. Numerical techniques are used to solve the equations either sequentially (segregated) or simultaneously (coupled) for new variable values. Domain initialization provides the starting values. Discrete coupled algebraic equations are first linearized by either the implicit or the explicit (only coupled) technique. For implicit segregated or coupled solver options, a point-implicit Gauss-Seidel linear equation solver is used in conjunction with an Algebraic Multigrid (AMG) method to solve for the dependent variables. For explicit coupled solver, a multi-stage (Runge-Kutta) solver is used to obtain the new variable values. A Full Approximation Storage (FAS) multigrid scheme is available as option for this case to accelerate solution convergence [31].

3. SIMULATION TEST CASES

All full-length plug nozzle contours are for an area ratio of 12. The design Mach number is 3.41.

3.1 Internal-External Expansion Axisymmetric Full-Length Contoured Plug Nozzle

Figure 1 shows that plug nozzle nicely occupies almost the whole launcher base area. It has many advantages. First, it substantially reduces the base drag. Second, nozzle can use the whole base area for flow expansion to very high area ratios.

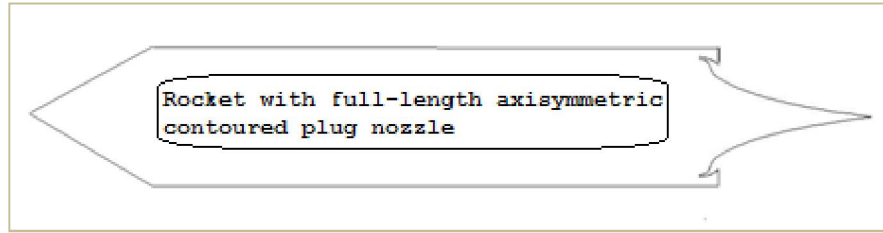


Figure 1: Rocket with full-length axisymmetric contoured plug nozzle

Figure 2 shows the flow domain. Nozzle geometry and grid have been generated in GAMBIT and exported as 2D mesh for further processing in FLUENT.

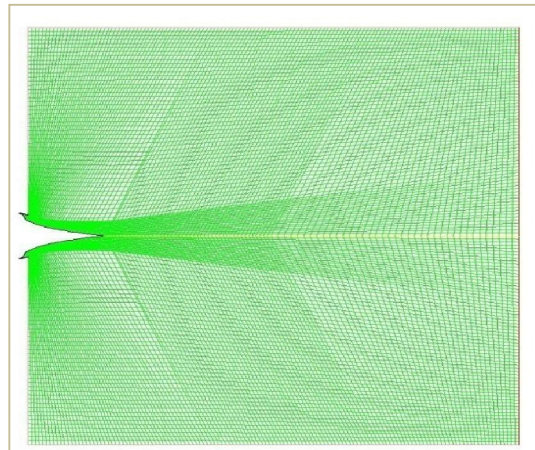


Figure 2: Grid for internal-external expansion full length contoured plug nozzle (inviscid)

Figure 3 profiles the Mach number contours. The maximum Mach number is in the hypersonic range and substantially deviates from the theoretical value of 3.41 at spike end. However, actual expansion up to the spike end is within the theoretical range.

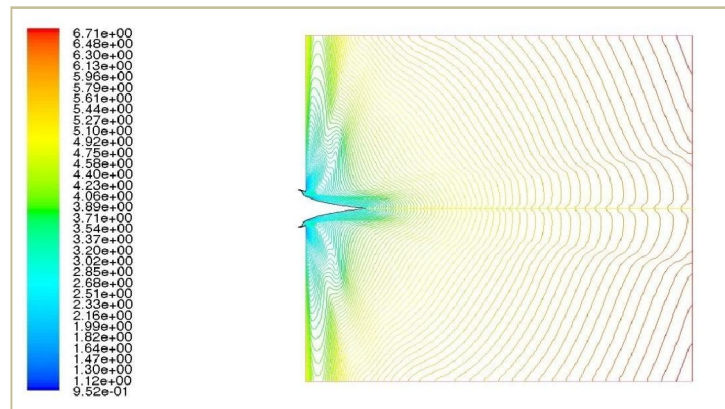


Figure 3: Mach number contours for full-length internal-external expansion plug nozzle (contoured)

Figure 4 indicates interesting trends in Mach number variation. On spike surface, the maximum Mach number is approximately 3.0 which is less than the theoretical value of 3.41. Moreover, a dip in Mach number (w-5 in Figure 4) indicates a shockwave on the spike at the exit of internal nozzle. Shockwave impinging on the spike surface is deviation from the ideal flow and subjects the surface to excessive heating. The spike profile developed following the procedure based on simple wave flow theory predicts flow that smoothly follows the spike contour generating no shockwave [28].

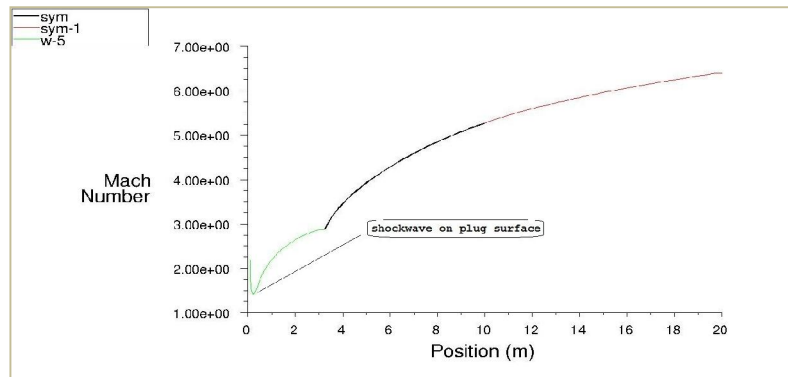


Figure 4: Plot for Mach number

3.2 External-Expansion Axisymmetric Full-Length Contoured Plug Nozzle

Figure 5 is rocket installed with external-expansion plug nozzle engine. Difficulty with this nozzle configuration is that the combustion chamber can't be easily installed into the engine aft body.

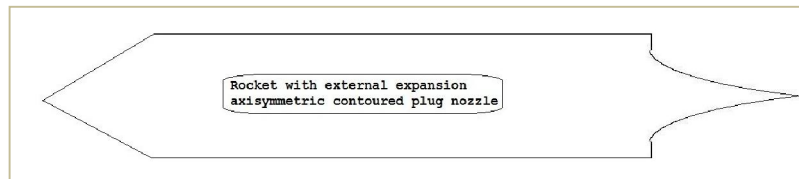


Figure 5: Rocket with external expansion axisymmetric contoured plug nozzle

Figure 6 is the case relevant grid showing some features of grid adaption in FLUENT [31, 32].

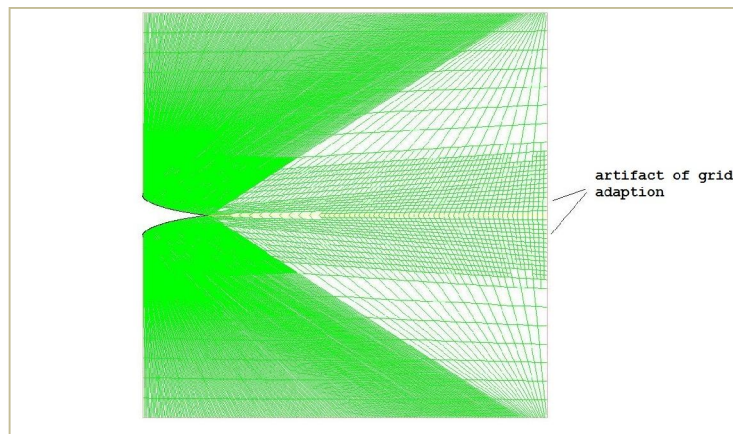


Figure 6: Grid adaption implemented in FLUENT

Figure 7 is the almost column-shaped exhaust plume characteristic of optimal flow expansion. However, the actual flow is slightly underexpanded. Maximum Mach number of 3.52 is near the theoretical value of 3.41.

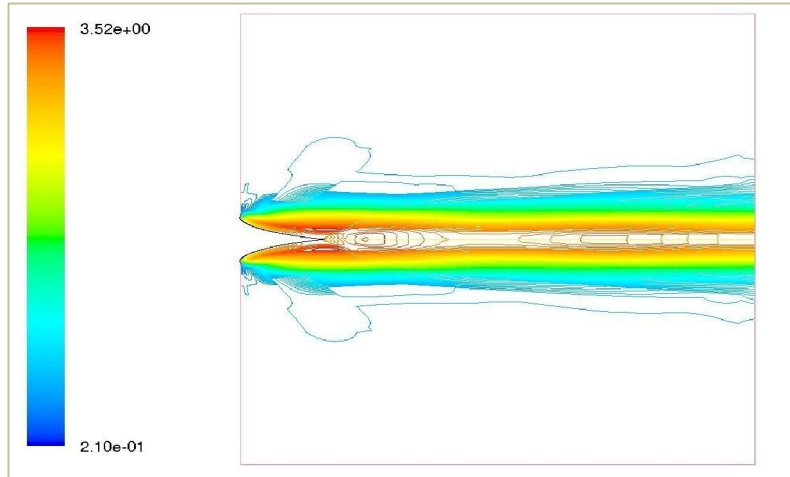


Figure 7: Mach number contours for adapted grid

Figure 8 is a smooth gradual decrease of static pressure along the spike surface.

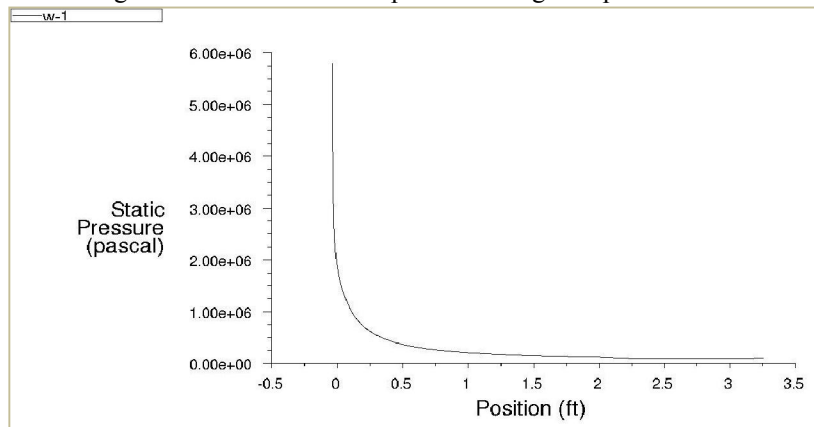


Figure 8: Full-length plug ramp, adapted grid (static pressure plot)

Figure 9 is the corresponding continuously increasing Mach number with no evidence of shockwave. Notice the peak value lies in the range 3.25-3.50.

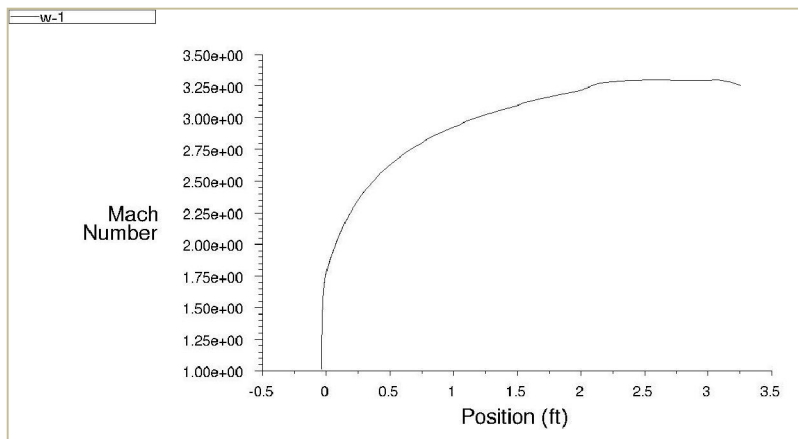


Figure 9: Full-length plug ramp, adapted grid (Mach plot)

3.3 External-Expansion Axisymmetric Truncated Contoured Plug Nozzle

Plug nozzle truncation is necessary to reduce spike length and weight [14, 32, 33] with a slight efficiency compromise [7]. Present case is for plug nozzle truncated at 1.2% of the full-length. Truncations at 10%, 20%, 30%, and 40%, however, are more common and feasible. Flowfield is showing many features in common with other similar flows.

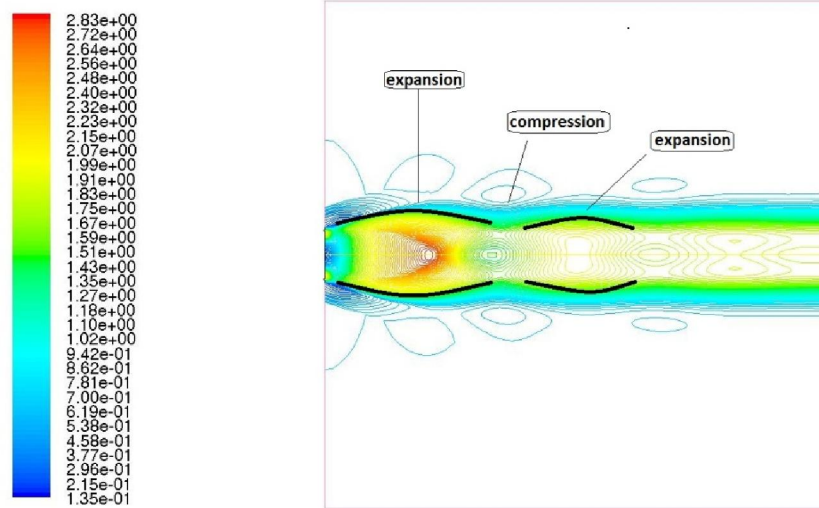


Figure 10: Nozzle exhaust plume expands and contracts

Figure 11 is set to show that there is no evidence of the pair of counter-rotating vortices at the nozzle base. Flow introduced at the bottom or somewhere in-between the bottom and the top of the nozzle base increases the thrust contribution by the base area.

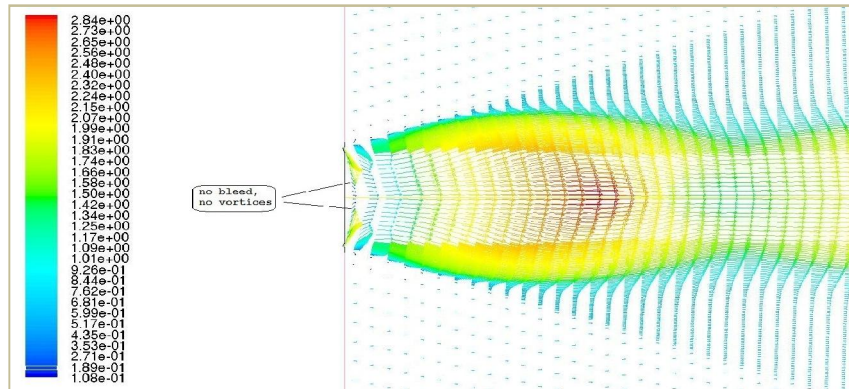


Figure 11: Contoured truncated plug nozzle- velocity vectors

3.4 Internal-External Expansion Axisymmetric Full-Length Conical Plug Nozzle

Flow at the internal nozzle exit is overexpanded in Figure 12. For the imposed boundary conditions and material properties it should be optimally expanded. The same data has been used for both the conical and the contoured cases. It shows that the contoured spike can't be converted to a conical form by the method used in the present case. However, present case needs further analysis for thrust comparison with the contoured spike.

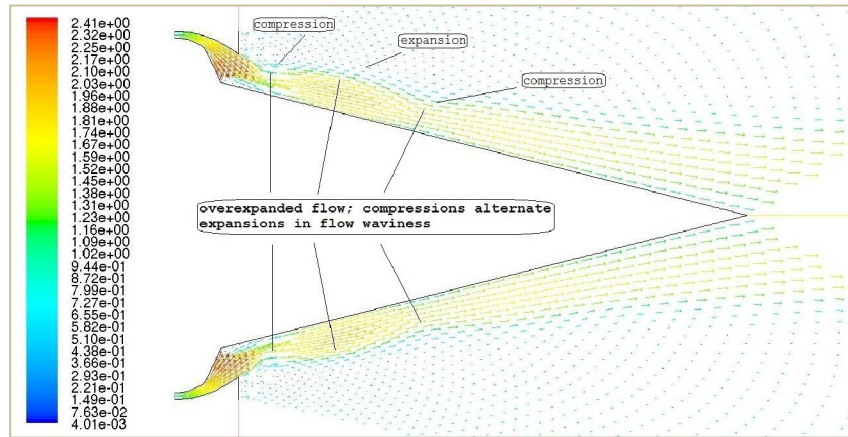


Figure 12: Conical plug nozzle (full-length)

Mach number plot in Figure 13 confirms the flow waviness on the conical spike surface. There is also a shockwave at the internal nozzle exit.

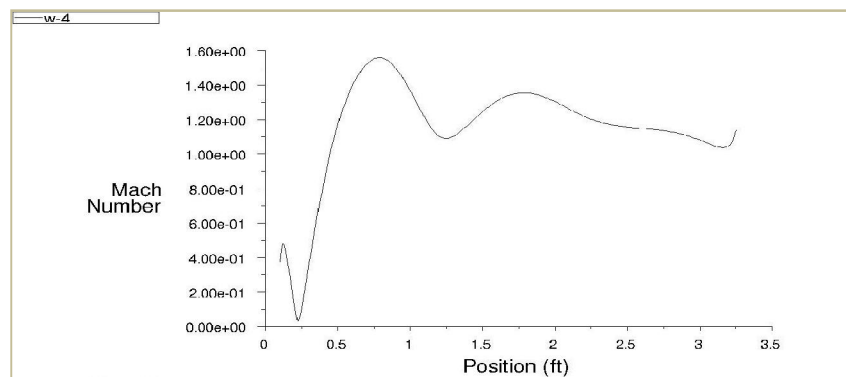


Figure 13: Mach number plot confirms undulating flow on plug surface

3.5 Internal-External Expansion Axisymmetric Truncated Conical Plug Nozzle

Figure 14 is just what goes into FLUENT along with boundary conditions and material properties.

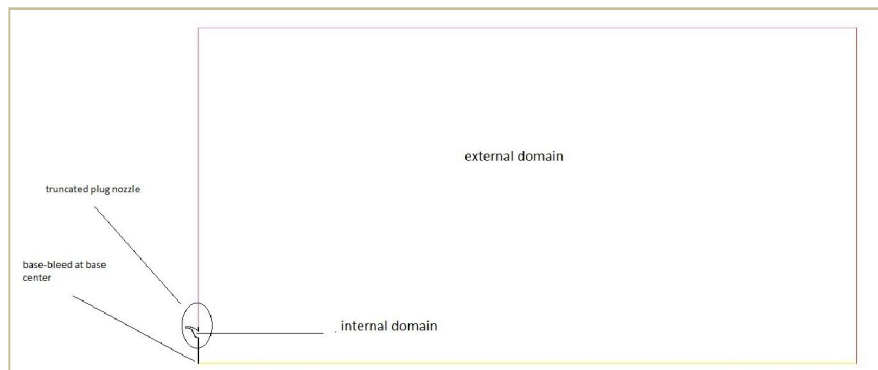


Figure 14: Internal-external expansion plug nozzle (truncated)

Figure 15 is part of the simulation task done in GAMBIT.

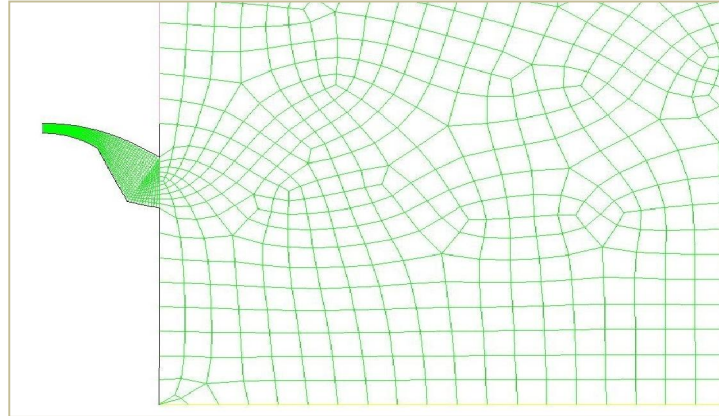


Figure 15: Grid for conical plug nozzle (truncated) in exploded view

Figure 16 is the manifestation of vortices due to flow induction at the center of the nozzle base. For the no-bleed case already discussed, there are no vortices. Given identical operating conditions, this nozzle type is reported to have reduced acoustic loading until wake closure compared to the full-length aerospike and the typical convergent-divergent nozzles [34].

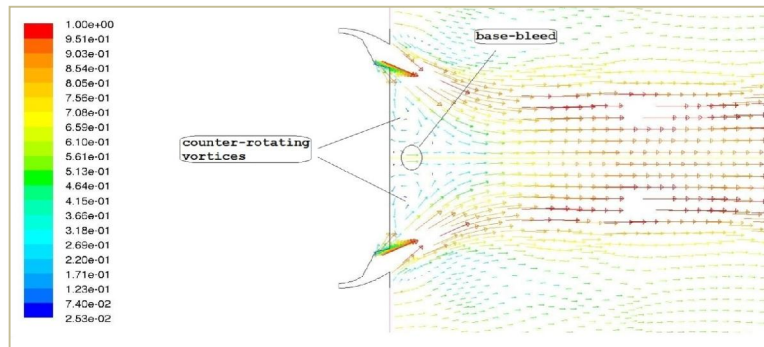


Figure 16: Base-bleed initiates counter rotating vortices

4. Results, Discussion and Recommendations

Mach number contours and plot (Figures 3 and 4) for the internal-external expansion axisymmetric full-length contoured plug nozzle confirm that the inviscid expansion process for this case is not in accordance with the theory prediction. Shockwave at the internal-nozzle exit distorts flow expansion downstream. Method of characteristics may solve this issue [7, 15]. However, Mach number contours, plots of static pressure and Mach number (Figures 7, 8 and 9) for the external-expansion axisymmetric full-length contoured plug nozzle closely follow the theoretical prediction. Uniform flow at the throat is ensured by the boundary conditions with fluid approaching the plug ramp as required. It flows smoothly along the ramp without any shockwave. Truncated plug nozzle (Figure 10) shows fascinating flow structures. Further investigation is required in this case. Underexpanded flow (Figure 12) for the internal-external expansion axisymmetric full-length conical plug nozzle indicates that converting a contoured plug nozzle by the present method doesn't automatically produce an efficient

nozzle and the same holds true (Figures 10 and 16) for the truncated plug nozzles [33, 35]. For the truncated case (Figure 16), one simulation result included here is for the effect of base-bleed. Counter-rotating vortices are the easily noticeable flow feature. This case requires further investigation.

5. CONCLUSIONS

Simulations of flowfield for the aerospike/plug nozzle configurations have been made using FLUENT for inviscid isentropic flow and compared with theoretical predictions. Theory and simulation results do not agree for internal-external expansion axisymmetric full-length contoured plug nozzle. Numerically simulated results in the case of external-expansion axisymmetric full-length contoured plug nozzle agree with theoretical analysis. Current contour design approach is adequate for this nozzle configuration. Internal-external expansion axisymmetric full-length conical plug nozzle performs poorly. Internal-external expansion axisymmetric

truncated conical plug nozzle shows flow with well-known counter-rotating vortices.

Acknowledgments

The first author is indebted to UET, Taxila, Pakistan, for academic, administrative and financial support. It would be unfair not to mention the eleventh-hour motivation provided by Professor Dr A. R. Ghumman.

Corresponding Author

Khalid Masood Khan
Mechanical Engineering Department
University of Engineering and Technology, Taxila,
Pakistan
E-mail: kmkhan89@yahoo.com

References

1. Verma, S. B. and Viji, M., "Linear-Plug Flowfield and Base Pressure Development in Freestream Flow," Vol. 27, No. 6, November–December 2011, Journal of Propulsion and Power.
2. Takashi, I. and Fujii, K., "Numerical Analysis of the Base Bleed Effect on the Aerospikes Nozzles," AIAA-2002-0512, January 2002, 40th AIAA Aerospace Sciences Meeting and Exhibit.
3. Verma, S.B., "Performance Characteristics of an Annular Conical Aerospikes Nozzle with Freestream Effect," Vol. 25, No. 3, May–June 2009, Journal of Propulsion and Power.
4. Ostlund, J. and Muhammad-Klingmann, B., "Supersonic Flow Separation with Application to Rocket Engine Nozzles," Applied Mechanics Reviews, 58, 143-177, 2005.
5. Mattingly, J. D. and Ohain, H. von (Forword), "Elements of Propulsion: Gas Turbines and Rockets," Education Series, © 2006 by AIAA.
6. Zhao, Q., Mo, J. D., Chow, A. S., and He, K. X., "Numerical Modeling of Aerospikes Nozzle Characteristics," AIAA 2000-3849, 16-19 May 2000, 36th AIAA/ASME/SAE/ASEE Joint Propulsion Conference & Exhibit.
7. Onofri, M., Calabro, M., Hagemann, G., Immich, H., Sacher, P., Nasuti, F., and Reijasse, P., "Plug Nozzles: Summary of Flow Features and Engine Performance," Overview of RTO/AVT WG 10 Subgroup 1, AIAA 2002-0584.
8. Corda, S., Neal B. A., Moes, T. R., Cox, T. H., Monaghan, R. C., Voelker, L. S., Corpening, G. P., Larson, R. R., and Powers, B. G., "Flight Testing the Linear Aerospikes SR-71 Experiment (LASRE)," NASA/TM-1998-206567.
9. Mori, H., Taniguchi, M., Nishihira, R., and Niimi, T., "Experimental Analyses of Linear-Type Aerospikes Nozzles with and without Sidewalls," AIAA 2005-1350, January 2005, 43rd AIAA Aerospace Sciences Meeting and Exhibit.
10. Wang, C.-H., Liu, Y., and Qin, L.-Z., "Aerospikes Nozzle Contour Design and its Performance Validation," Acta Astronautica, Vol. 64, 2009, pp. 1264-1275.
11. Ito, T., Fujii, K., and Hayashi, A. K., "Computations of the Axisymmetric Plug Nozzle Flow Fields- Flow Structures and Thrust Performance," AIAA-99-3211, 28 June-1 July 1999, 17th AIAA Applied Aerodynamics Conference.
12. Hagemann, G., Immich, H., Nguyen, T. V., and Dumnov, G. E., "Advanced Rocket Nozzles," Journal of Propulsion And Power, Vol. 14, No. 5, September–October 1998.
13. Ruf, J. H. and McConnaughey, P.K., "The Plume Physics Behind Aerospikes Nozzle Altitude Compensation and Slipstream Effect," AIAA-97-3218.
14. Sule, W. P., and Mueller, T. J., "Annular Truncated Plug Nozzle Flowfield and Base Pressure Characteristics," AIAA Paper No. 73-137, JANUARY 1973, 11th AIAA Aerospace Sciences Conference.
15. Hagemann, G., et al., "Flow Phenomena in Advanced Rocket Nozzles - The Plug Nozzle," AIAA paper 98-3523, 1998.
16. Geron, M., et al., "Analysis of a Three-Dimensional Flow Generated by a Linear Aerospikes," AIAA 2005-3231, May 2005, AIAA/CIRA 13th International Space Planes and Hypersonics Systems and Technologies Conference.
17. Panossian, H., et al., "Aerospikes Engine Control System Features and Performance," 17-19 July 2000, AIAA/ASME/SAE/ASEE Joint Propulsion Conference.
18. Wood, D., Landrum, B., and Demaneuf, O., "Analysis of the Rocket Plug Nozzle Combined Cycle Propulsion System," AIAA 2008-5168, 21 - 23 July 2008, 44th AIAA/ASME/SAE/ASEE Joint Propulsion Conference & Exhibit.
19. Shen, L., et al., "Ducts and Lines of the XRS-2200 Linear Aerospikes Rocket Engine," AIAA- 99-2186, 20-24 June 1999, 35th AIAA/ASME/SAE/ASEE Joint Propulsion Conference and Exhibit.
20. Wisse, Menko E. N., et al., "Analytical Optimisation of an Inviscid Flow Linear Plug Nozzle Boattail," AIAA 2004-4017, 11 - 14 July 2004, 40th AIAA/ASME/SAE/ASEE Joint Propulsion Conference and Exhibit.
21. Rommel, T., et al., "Plug Nozzle Flowfield Analysis," Journal of propulsion and power, 13 (5), 629-634, 1997.

22. Griffith, A. A., "Jet Propulsion Nozzle for Use at Supersonic Jet Velocities [P]," American Patent Number 2683962, Rolls-Royce Limited, July 20, 1954.
23. Dymond, T. L., "A Simplified Method for Plug Nozzle Design," Technical Memorandum No. 140, July, 1960.
24. Eilers, Shannon D., et al., "Side Force Amplification on an Aerodynamically Thrust Vectored Aerospike Nozzle," AIAA 2011-5531, 31 July - 03 August 2011, 47th AIAA/ASME/SAE/ASEE Joint Propulsion Conference & Exhibit.
25. Onofri, M., et al., "Plug Nozzles: Summary of Flow Features and Engine Performance," Overview of RTO/AVT WG 10 Subgroup 1, AIAA Paper No. 02-0584, January 2002.
26. Hagemann, G., et al., "Critical Assessment of the Linear Plug Nozzle Concept," AIAA Paper 2001-3683, July 2001, 37th AIAA/ASME/SAE/ASEE Joint Propulsion Conference & Exhibit.
27. Wilson, A., et al., "CFD Analysis of a Multi-Chamber Aerospike Engine in Over-Expanded, Slipstream Conditions," AIAA 2009-5486, August 2009, 45th AIAA/ASME/SAE/ASEE Joint Propulsion Conference & Exhibit.
28. Lee, C. C., "Fortran Programs for Plug Nozzle Design," NASA Technical Note R-41, March 1963.
29. Lee, C. C. and Thompson D. D., "Fortran Program for Plug Nozzle Design," NASA TM X-53019, 1964.
30. Temam, R., "Navier-Stokes Equations and Nonlinear Functional Analysis," CBMS 41, SIAM, Philadelphia, PA, 1983.
31. FLUENT 6.2 User's Guide, January 2005.
32. Bristeau, M.O., Glowinski, R., and Periaux, J., "Numerical Methods for the Navier-Stokes Equations. Applications to the Simulation of Compressible and Incompressible Viscous Flows," Computer Physics Reports 6 (1987) 73-187, North-Holland, Amsterdam, 0167-7977/87 © Elsevier Science Publishers B.V. (North-Holland Physics Publishing Division)
33. Ladeinde, T. and Chen, H., "Performance Comparison of a Full-Length and a Truncated Aerospike Nozzle," AIAA 2010-6593, 25- 28 July 2010, 46th AIAA/ASME/SAE/ASEE Joint Propulsion Conference & Exhibit.
34. Karthikeyan, N., Kumar, A., Verma, S. B., and Venkatakrishnan, L., "Effect of Spike Truncation on the Acoustic Behavior of Annular Aerospike Nozzles," AIAA Journal: 1-15, Posted online on 26 July 2013. doi: 10.2514/1.J052139.
35. Rao, G. V. R., "Spike Nozzle Contours for Optimum Thrust," Ballistic Missiles and Space Technology, Vol. 2, C. W. Morrow (Ed.), Pergamon Press, New York, 1961.

7/23/2013